

Fetter Model Revisited: Detecting Nuclear Weapons 30 Years Later

Moritz Kütt*, Jan Elfes*, Christopher Fichtlscherer*,†

* Institute for Peace Research and Security Policy at the University of Hamburg, Hamburg, Germany

† Rheinisch-Westfälische Technische Hochschule Aachen, Aachen, Germany

Contact: kuettt@ifsh.de

**Proceedings of the INMM & ESARDA Joint Virtual Annual Meeting
August 23-26 & August 30-September 1, 2021**

Abstract: Current nuclear arms control agreements include mechanisms to verify numerical limits of deployed strategic nuclear weapons. Future disarmament agreements will likely rely on approaches to authenticate nuclear weapons and to demonstrate their dismantlement. Both types of agreements could benefit from reliable ways of detecting nuclear weapons at a distance - or showing that they are absent from a facility or larger site.

Revisiting a public notional weapon model created by Fetter et al. in 1990, we use the Open Source Monte Carlo code OpenMC to simulate the detection of passive neutron emissions from plutonium-based weapons. The distance from which these types of weapons can be detected depends on two aspects: Firstly the neutron absorption and the scattering in materials between the weapon and detector (e.g., container or shielding), and secondly the ability of a measurement system to discriminate between the signal and the cosmic-ray neutron background. We analyze potential neutron detection systems and estimate detection ranges for plausible nuclear weapon deployment and storage scenarios based on simulations.

1 Introduction

Today, experts estimate global nuclear weapon stockpiles to include 13,100 warheads [1]. Arms control agreements limiting the number of these weapons, as well as disarmament agreements seeking to reduce the stockpiles, create the need for comprehensive verification mechanisms. Commonly discussed verification approaches enable inspectors to authenticate objects as nuclear weapons, to track weapon components through the dismantlement process (chain-of-custody) or to prevent the diversion of weapon-origin fissile material. Rarely discussed, but potentially relevant, are reliable ways to detect nuclear weapons from a distance.

Any nuclear weapon-usable isotopes are radioactive. Hence, nuclear weapons inevitably emit some gamma and neutron radiation. This article revisits the issue of passive warhead detection from a distance using modern simulation tools. It addresses two main questions: 1) What are

the neutron emissions of a notional nuclear weapon? 2) At what distances can measurements reliably show the presence/absence of nuclear weapons? Clearly, answers to both questions depend on a large number of parameters. Different types of nuclear weapons will create different neutron emissions, different environments will influence the detection range.

This article should be the start of a larger research project studying ways to detect neutrons from a distance. It builds upon previous work that discussed the detection of nuclear weapons and fissile material (cf. [2–6]). Here, we focus first on passive measurements alone.

One particular application of measurements capable to detect nuclear weapons is to demonstrate the absence thereof. As part of New START, neutron measurements can be used to “demonstrate to inspectors that an object located on the front section of a deployed ICBM or deployed SLBM and declared by a member of the in-country escort to be a non-nuclear object, is, in fact, non-nuclear;” [7, Section VI, paragraph 1(a)]. Recently, multiple researchers proposed new disarmament verification schemes focusing initially or as a whole on the absence of weapons [8, 9]. A team at Princeton University proposed a method to demonstrate the absence of nuclear weapons through the measurement of gamma radiation [10]. Demonstrating the absence of nuclear weapons has the benefit that it does not require the measurement of sensitive information to ensure compliance.

The article proceeds as follows: In the next section, the neutron emission intensity and energy spectra of a notional nuclear warhead is presented. Section 3 discusses neutron background resulting from cosmic rays and simple measurement scenarios. Two more complex detection scenarios with notional warhead deployment sites are presented in Section 4. Detailed scripts to reproduce the results are provided at <https://github.com/ohnemax/inmm2021-nukeview/>.

2 Neutron Emissions from a Nuclear Warhead

In the late 1980s, intensive cooperation took place between Soviet and American research institutions. U.S. scientists visited a Soviet nuclear test site to install seismic detectors [11]. Collaboration continued with a large study on arms control verification mechanisms [2] and culminated 1989 in the visit of American scientists to measure radiation signatures of a Soviet nuclear weapon as part of the “Black-Sea Experiment” [12, 13].

As part of this cooperation, a group of scientists proposed a simple model of a notional implosion-type nuclear weapon. The model is commonly called “Fetter Model”, after the first author of the paper in which it was first presented [3]. Figure 1 shows the model consisting of concentric spheres of material. To estimate the neutrons emitted by this weapon, we use the Monte Carlo particle transport software OpenMC [14]. The open source software allows for simulations of 3-dimensional geometries with fixed source terms, and to estimate (“tally”) physical properties, e.g. outgoing neutron current. The simulations use the neutron interaction cross section library ENDF-VIII.0. The composition of the 4 kg of weapon-grade plutonium is taken from [3]. All other material compositions and densities are taken from [15].¹

¹[3] lists four different warhead models, we study the plutonium model with a tungsten tamper.

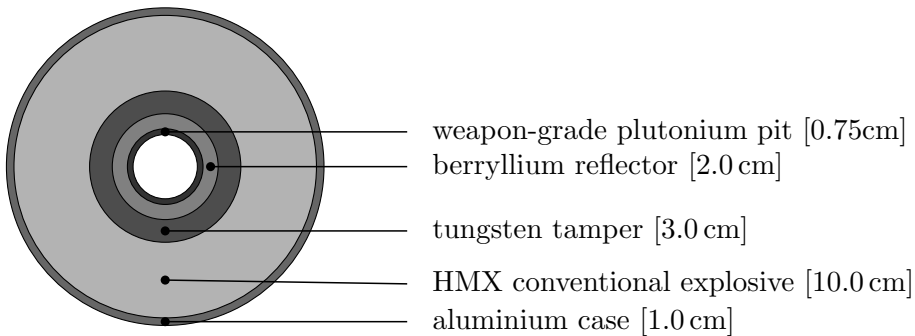


FIGURE 1: Notional nuclear weapon model. The values in brackets describe the thickness of each shell. The plutonium shell has an outer radius of 5 cm.

Two different mechanisms exist to produce initial neutrons from radioactive decay. First, spontaneous fission events produce neutrons with energies similar to neutrons from induced fission. Second, alpha decay, which in turn produces neutrons through (α, n) reactions in low-Z materials. Although [3] discusses minor oxygen impurities in the model, these are ignored here as their contributions are negligible.

The rates of neutrons produced per isotope are listed in table 1. Half-lives, spontaneous fission branching ratios and average neutrons per spontaneous fission are based on recently published values. We find that plutonium-240 emits 1031 neutrons/s, a figure approx. 10 % larger than the 910 neutrons/s given in [3]. Differences for other isotopes are smaller, mostly below 1 %. Based on the data in Table 1, in a pit of 4 kg weapon-grade plutonium 249 100(8600) neutrons/s are produced by radioactive decay (about 10% more than the 224,000/s in [3]).

From the simulations of the model, we calculate the effective multiplication factor

$$k_{eff} = \frac{\text{additional neutrons produced}}{\text{neutrons absorbed} + \text{neutrons leaked}} = 0.626(6) \quad (1)$$

TABLE 1: Reference values for half-life, spontaneous fission branching ratio and average neutrons per spontaneous fission. Fission/neutron rates calculated based on other listed values.

	$T_{1/2}$ * [years]	Branching Ratio *	fission rate [fissions/g/s]	$\bar{\nu}$ †	neutron rate [neutron/g/s]
^{238}Pu	87.7(1)	$1.9(1) \times 10^{-9}$	1204(63)	2.187	$2.63(14) \times 10^3$
^{239}Pu	$2.441(3) \times 10^4$	$3.1(6) \times 10^{-12}$	0.0070(14)	2.16	0.0152(29)
^{240}Pu	6561(7)	$5.7(2) \times 10^{-8}$	479(17)	2.154	1031(36)
^{241}Pu	14.329(29)	2×10^{-16}	0.000 765 9(16)	2.25	0.001 723 3(35)
^{242}Pu	$3.75(2) \times 10^5$	$5.50(6) \times 10^{-6}$	801.5(97)	2.149	1722(21)
^{241}Am	432.6(6)	$3.6(9) \times 10^{-12}$	0.46(11)	3.22	1.47(37)

* ^{238}Pu [16], ^{239}Pu [17], ^{240}Pu [18], ^{241}Pu , ^{241}Am [19], ^{242}Pu [20].

† Calculated from [21].

The simulations used 100 million start particles. To estimate the number of neutrons produced, OpenMC offers two special tally scores, `nu-fission` and `nu-scatter`. The first returns the number of neutrons produced in fission events. The second returns neutrons resulting from inelastic scattering events, including other multiplying reactions like (n, 2n) and (n, 3n). A surface current tally through a cube surface around the weapon model estimates neutron leakage, a tally using the `absorption` score the rate of absorptions. From the multiplication factor, we calculate the geometry's multiplication as

$$M = \frac{1}{1 - k_{eff}} = 2.67(4) \quad (2)$$

The result is significantly higher than the result of Fetter et al. (1.89) [3]. Calculated as outlined above, the multiplication describes the total number of neutrons produced in a sample per starting neutron. However, not all of these neutrons leave the sample. A significant fraction is also lost to absorption reactions. To describe the number of neutrons leaking per neutron produced, one can use M_L , the leakage multiplication:

$$M_L = p_L \cdot M \quad (3)$$

Here, p_L describes the probability of a neutron to leak. In our case, the result of the outer surface current tally directly yields $M_L = 0.8007(1)$. Hence, we find that in total, the system emits 199 400(6900) neutron/s. As can be seen in Figure 2, multiplication takes place mostly in the weapon-grade plutonium pit. Two thirds of the neutrons leaving the tamper in outward direction are either absorbed in or reflected by the high explosive. Fetter et al. find a total leakage of 400,000 neutron/s. Likely, the total multiplication was taken as the leakage multiplication or the absorption in the high explosive was estimated to be smaller.

Figure 2 also shows the initial energy distribution of source neutrons, and the resulting energy distribution emitted by the assembly. Most of the moderation to thermal energies takes place in the conventional explosive.

3 Cosmic-Ray Neutron Background

The earth is continuously bombarded with high energy particles originating from both the sun and other galactic sources. Particles include mainly protons and alpha particles, and a small fraction of heavier atoms as well as gammas. Through spallation reactions with nuclei in the atmosphere, the incoming particles create secondary particles, for example pions, muons and neutrons. The relevant secondary particles on the ground influencing particle measurements are muons and neutrons.

Kouzes et al. [22] provide a literature review of the intensity of the neutron background. Referred studies range from 40 neutrons/(s·m²) to 200 neutrons/(s·m²) and recommend a value of 120 neutrons/(s·m²). Fetter et al. assume an intensity of 50 neutrons/(s·m²) [3].

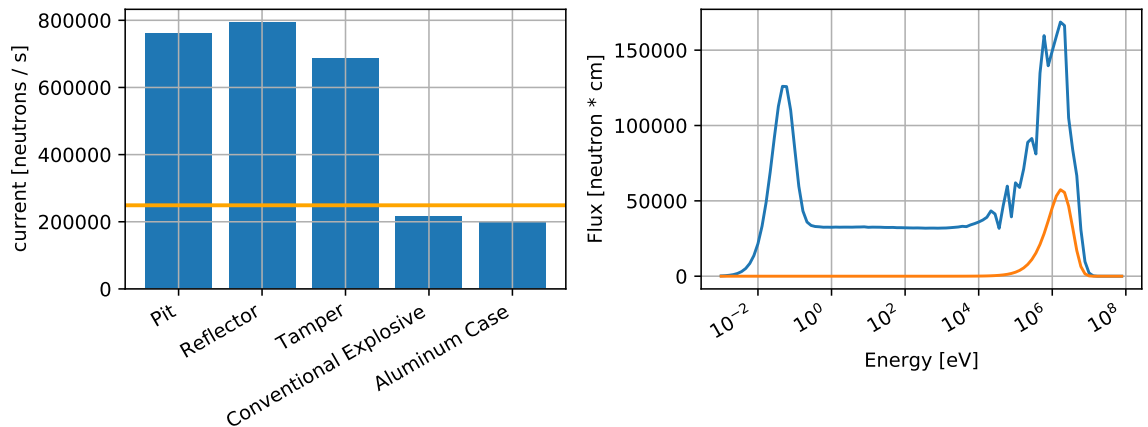


FIGURE 2: Left: Total neutron current leaving respective simulation cells through outer surface. The orange horizontal line shows the number of neutrons/s started from radioactive decay. Right: Neutron energy distribution for neutrons leaving the notional weapon model. The orange line shows the energy distribution for neutrons from radioactive decay (arbitrary y-axis).

Muons arrive with an intensity of approx. $167 \text{ muons}/(\text{s}\cdot\text{m}^2)$ [23]. The solar component of the primary cosmic rays is subject to changing patterns with diurnal, annual and 11-year cycles. Besides interactions in the atmosphere, both primary and secondary particles also interact with solid materials, producing additional particles. This “ship effect” becomes particularly relevant for measurements within buildings.

To allow for the estimation of neutron background around buildings, we used the Cosmic-Ray Shower Library [24]. The library itself provides a quadratic surface particle source emitting neutrons with energies and directions corresponding to expected values. For the following simulations, the library was used as a particle source for OpenMC through the “custom source” feature.² A special neutron cross section library (JENDL 4.0/HE) allowed for simulation with neutron energies up to 200 MeV. The small fraction of neutrons with higher energies has been discarded in the simulations.

First, simple simulations of a 200 m by 200 m square were carried out. The simulations include a ground layer of 5 m thickness (either as soil, concrete or water), and an air layer of 10 m thickness. A single nuclear weapon is placed at a height of 1.5 m above the ground in the center of the square. Through particle current tallies, we estimated the number of neutrons entering each 1 m^3 volume in the simulated geometry. The cosmic-ray source was placed at the top of the air layer. Simulations with cosmic-ray sources and the nuclear weapon as a source were carried out separately. For each simulation, 200 million particles were started. Tally results for cosmic rays are multiplied with a constant to achieve an average source neutron current of $120 \text{ neutrons}/(\text{s}\cdot\text{m}^2)$, tally results with a nuclear weapon are multiplied with the source term determined in the previous section.

²Further information on the source, including a reusable shared library, can be found at <https://github.com/ohnemax/cry-with-openmc>.

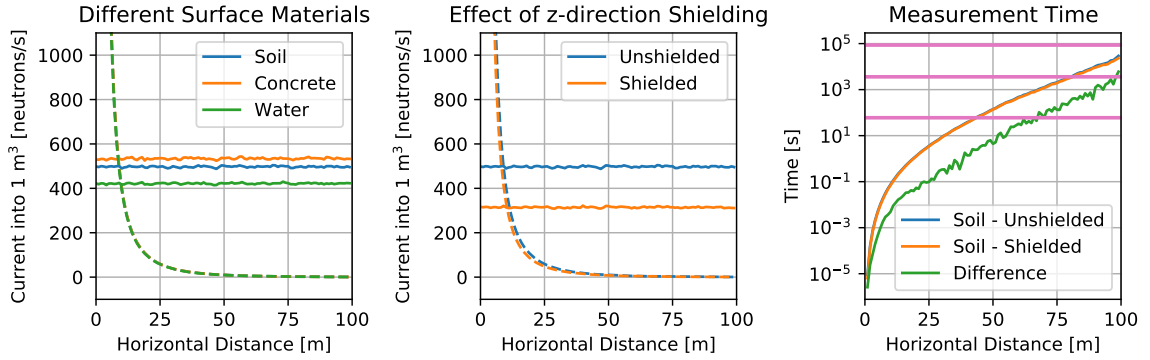


FIGURE 3: Left/Center: Neutron currents in 1 m^3 volumes resulting from cosmic-ray neutron background (solid lines) and a single nuclear weapon (dashed lines). The volumes are at the height of the weapons (between 1 m and 2 m above ground). Left: Comparison of different ground materials. Center: Comparison of neutron current from all directions (“unshielded”) with current only from x- and y-directions (“shielded”). Right: Measurement time required to distinguish weapon emissions from background (for 5 standard deviations). The pink lines show 1 minute, 1 hour and 1 day time limits.

Figure 3 shows resulting particle currents in the volumes in positive x-direction from the nuclear weapon. The figure on the left shows that different ground materials have different reflecting and multiplying effects, lowest for water and highest for concrete. All increase the total neutron current in the air. Neutron interaction with ground materials have negligible effects on the neutron emissions from a nuclear weapon. Already at a distance of 10 m, neutron currents are of equal level, assuming a similar detector area facing both sources.

The center image in Figure 3 indicates the effect of “shielding.” In the “shielded” case, only neutrons entering the volume through the sides, not from top or bottom, are accounted for. This simple improvement leads to a decrease of incoming background neutrons by approx. one third of the total value. It becomes clear that a significant fraction of background neutrons does not travel perpendicular to the surface. The reduction of the weapon signal is small.

To detect the nuclear weapon, however, both signals do not need to be equal. As long as the background signal can be reliably determined, measurement times can be adjusted to ensure that the contribution of the additional signal is larger than an anticipated measurement uncertainty. Using S_W as the weapon source signal and S_C as the cosmic-ray source signal, the following condition should be met:

$$S_W \cdot t > m \sqrt{S_C \cdot t} \quad (4)$$

In the equation, m describes the number of standard deviations that the weapon signal must exceed. Here, we require that the signal is larger than 5 standard deviations. The right image of Figure 3 shows that within an hour, the criteria can be met up to a distance of 75 m. The image again compares “shielded” and “unshielded” detectors. The effect on measurement time, however, is small. Shielding only brings a 10 % reduction in measurement times.

4 Deployment Scenarios

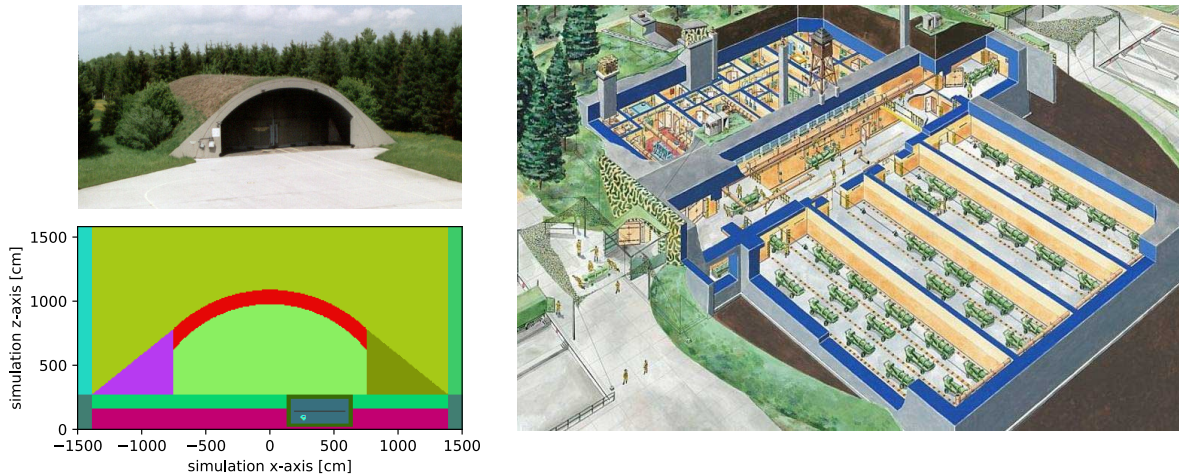


FIGURE 4: Top left: Protective aircraft shelter at Büchel airbase (Germany), photo by Sphynx2503, Wikimedia Commons, CC-BY 3.0. Bottom left: OpenMC implementation of the aircraft shelter, xz-cut through the underground vault, including the notional nuclear weapon assembly. Right: Schematic of a former Soviet weapon storage bunker. Copyright: Robert Jurga, reprinted with permission.

In typical inspection scenarios, inspectors will try to determine the presence or absence of nuclear weapons in buildings, storage sites or bunkers. To illustrate the increased complexity, we simulated two different deployment scenarios, both shown in Figure 4. First, we simulate the notional nuclear weapon inside a protective aircraft shelter (PAS). Such a deployment scenario is currently in active use in Germany, which hosts 15-20 American nuclear weapons at the Büchel airbase. Dimensions were derived using openly accessible photos and satellite imagery. Typically, up to four B61 gravity bombs can be stored inside an underground vault. For the simulations presented here, a single assembly according to the description previously is placed in the lower part of the vault. Second, we simulate a larger weapon storage bunker that was commonly used by the Soviet Union to store forward-deployed weapons in Warsaw Pact countries. The bunker consists of four underground chambers for warhead storage, a crane hall where weapons can be lowered into the chambers and an auxiliary building. The dimensions are derived from the image shown in the figure. A single weapon is placed at the end of one of the chambers. The whole bunker is covered with soil.

Without detailed design information, the models use simple material compositions. Walls and ceilings are made out of reinforced concrete, assuming a steel fraction of 300 kg per m^3 of material. Doors are simulated as plain steel doors. All doors are assumed to be closed. For both deployment scenarios, we assume a total footprint of 200m by 200m. Simulations with cosmic-ray sources and the nuclear weapon as a source were carried out separately. For the background case, vertical surfaces are modeled as periodic surfaces. 500 million particles were simulated for the background case. For the weapon case, the use of the `SURVIVAL_BIASING` setting of OpenMC increases the computation efficiency (neutron cut-off weight: 0.05). 2 bil-

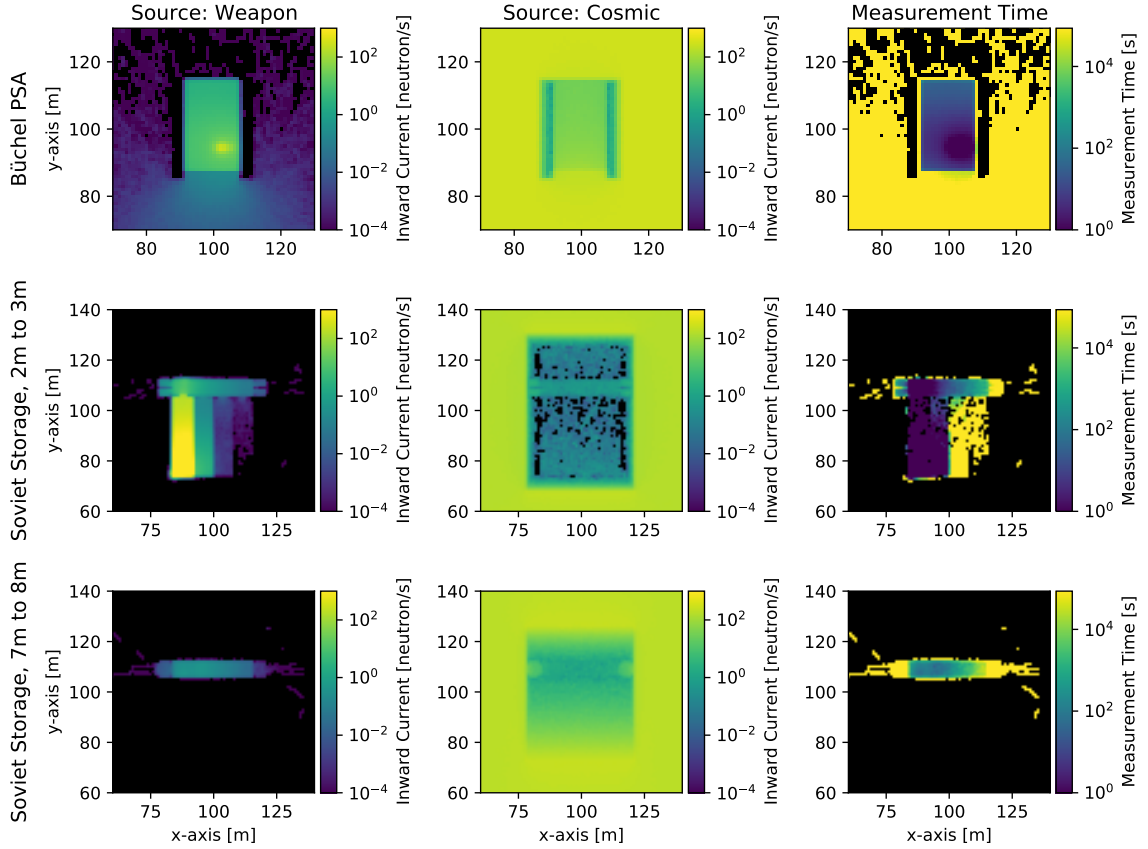


FIGURE 5: Selected results from simulations of the Büchel PSA and the Soviet weapon storage. The left column shows neutron currents in 1 m^3 volumes resulting from a single weapon. The center column shows neutron currents in 1 m^3 volumes from cosmic-ray neutron background. Both currents do only consider the four vertical surfaces (“shielded”). The right column shows measurement times for which the weapon signal equals three standard deviations of the background signal. Black pixels show volumes where no signal could be generated within the simulations.

lion particles were simulated for this case. To determine the detectability, a mesh surface tally with cells of volume 1 m^3 is used.

Key results of these simulations are shown in figure 5. Clearly, detecting warheads from the outside of hardened buildings is nearly impossible. As seen in the right column of plots, required measurement times are longer than a full day for most locations (here calculated for only three standard deviations of the background). Only directly in front of the steel door of the PAS in Büchel, a detector could pick up the signal of a nuclear weapon within multiple hours. Interestingly, measurement times are further reduced at levels higher above ground. Background neutrons interact with the building materials, leading to a distortion of the average background in the near field of each structure. Due to this facts, inspectors will have to take great care to determine the expected background levels. For the Soviet storage

site, a detection from the outside is impossible. The traces outside of the facility result from very few individual neutrons.

The situation improves inside of the buildings, as they shield the neutron background. Inside of the PSA in Büchel, measurement times of less than 100 seconds are sufficient. In addition, assuming the bunker structure to be homogeneous, the presence of the weapon (point source) could also be detected by measuring at multiple locations (cf. top left plot of figure 5).

Rarely any neutron background enters the base level of the Soviet storage facility. In the hallway, very short measurements (seconds) could demonstrate the absence or presence of a nuclear weapon. At the level of the crane hall, through which warheads enter or leave the facility, some background is present. Still, the presence of a weapon can be detected within a few hundred seconds. Thick steel doors, however, block any signal leaving the facility.

5 Conclusion

In this article, we set out to revisit the calculations by American and Soviet scientists in the late 1980ies on detectability of nuclear weapons. We find that plutonium weapons emit approx. 200,000 neutrons/s, significantly lower emission levels than previously presented. At the same time, the calculations here present higher neutron backgrounds. Still, we can show that detection from a distance is in principle possible. For deployment sites, especially those with hardened structures, individual warhead signatures inside are very well shielded when measuring outside. Indoor measurements – if allowed – seem feasible, but will increase inspection resources necessary to show the absence of weapons in large areas.

Future work studying this issue could proceed along various lines. First, research could focus on better discrimination between background and weapon signatures. Therefore, simple counting information could be supplemented with correlation information, energy information and finer grained directional information. Information from measurements at different locations could be combined, too. Second, background particles, in particular muons, could be used to probe both the surrounding structures as well as to search for fissile materials. Such approaches have been proposed in the past, mostly for detection of fissile material in cargo, but could be expanded to cover deployment sites similar to those discussed here. Third, active interrogation with transportable neutron sources could be studied. Again, they could be used to find weapons directly, but also to gain information on surrounding materials.

Besides first results, the presented work provides a framework for future analysis. We tried to provide detailed descriptions of our calculations, and presented them in a reproducible manner. This should help others to further study the issue of nuclear disarmament verification, and in particular the detection of the presence or absence of nuclear weapons.

References

- [1] H. Kristensen and M. Korda. *Status of World Nuclear Forces*. Federation Of American Scientists. URL: <https://fas.org/issues/nuclear-weapons/status-world-nuclear-forces/> (visited on 07/26/2021).
- [2] F. von Hippel and R. Z. Sagdeev, eds. *Reversing the Arms Race: How to Achieve and Verify Deep Reductions in the Nuclear Arsenals*; Science & Global Security / Monograph Series 1. New York: Gordon and Breach Science Publ., 1990.
- [3] S. Fetter, V. A. Frolov, M. Miller, R. Mozley, O. F. Prilutsky, S. N. Rodionov, and R. Z. Sagdeev. “Detecting Nuclear Warheads”. In: *Science & Global Security* 1.3-4 (1990), pp. 225–253. DOI: 10.1080/08929889008426333.
- [4] S. Belyaev, V. Lebedev, B. Obinyakov, M. Zemlyakov, V. Ryazantsev, V. Armashov, and S. Voshchinin. “The Use of Helicopter-Borne Neutron Detectors to Detect Nuclear Warheads in the USSR-US Black Sea Experiment”. In: *Science & Global Security* 1.3-4 (1990), pp. 328–333. DOI: 10.1080/08929889008426339.
- [5] G. W. Phillips, D. J. Nagel, and T. Coffey. *A Primer on the Detection of Nuclear and Radiological Weapons*. Center for Technology and National Security Policy, National Defense University, 2005.
- [6] R. Maurer et al. *Aerial Neutron Detection: Neutron Signatures for Nonproliferation and Emergency Response Applications*. DOE/NV/25946–1634, 1136549. Oct. 17, 2012, DOE/NV/25946–1634, 1136549. DOI: 10.2172/1136549. URL: <http://www.osti.gov/servlets/purl/1136549/>.
- [7] *New START Treaty Protocol: Annex on Inspection Activities, Part Five - Inspection Equipment and Electronic Equipment Necessary for Inspectors*. 2010. URL: <https://www.acq.osd.mil/asda/iipm/sdc/tc/nst/annexes/NSTprotocolAnnexPartFive.htm> (visited on 07/27/2021).
- [8] P. Podvig, R. Snyder, and W. Wan. *Evidence of Absence: Verifying the Removal of Nuclear Weapons*. United Nations Institute for Disarmament Research, 2018.
- [9] A. Glaser. “Monitoring Regimes for All-Warhead Agreements”. In: *Toward Nuclear Disarmament: Building up Transparency and Verification*. Ed. by M. Götsche and A. Glaser. Berlin: German Federal Foreign Office, 2021, pp. 34–53. URL: <https://tinyurl.com/ebw97j8w>.
- [10] E. Lepowsky, J. Jeon, and A. Glaser. “Confirming the Absence of Nuclear Warheads via Passive Gamma-Ray Measurements”. In: *Nuclear Instruments and Methods in Physics Research Section A: Accelerators, Spectrometers, Detectors and Associated Equipment* (Dec. 26, 2020), p. 164983. DOI: 10.1016/j.nima.2020.164983.
- [11] W. J. Broad. “Westerners Reach Soviet to Check Atom Site”. In: *The New York Times. U.S.* (July 6, 1986). URL: <https://www.nytimes.com/1986/07/06/us/westerners-reach-soviet-to-check-atom-site.html>.
- [12] S. Fetter, T. B. Cochran, L. Grodzins, H. L. Lynch, and M. S. Zucker. “Gamma-Ray Measurements of a Soviet Cruise-Missile Warhead”. In: *Science* 248.4957 (May 18, 1990), pp. 828–834. DOI: 10.1126/science.248.4957.828.
- [13] T. B. Cochran. *Black Sea Experiment*. Natural Resources Defense Council, 2011. URL: https://www.nrdc.org/sites/default/files/nuc_11020401a.pdf (visited on 10/01/2019).
- [14] P. K. Romano, N. E. Horelik, B. R. Herman, A. G. Nelson, B. Forget, and K. Smith. “OpenMC: A State-of-the-Art Monte Carlo Code for Research and Development”. In: *Annals of Nuclear Energy* 82 (Aug. 2015), pp. 90–97. DOI: 10.1016/j.anucene.2014.07.048.
- [15] R. McConn Jr, C. J. Gesh, R. T. Pagh, R. A. Rucker, and R. Williams III. *Compendium of Material Composition Data for Radiation Transport Modeling*. PNNL-15870 rev. 1 4. Pacific Northwest National Laboratory, 2011.
- [16] E. Browne and J. Tuli. “Nuclear Data Sheets for a = 238”. In: *Nuclear Data Sheets* 127 (2015), pp. 191–332. DOI: 10.1016/j.nds.2015.07.003.
- [17] E. Browne and J. Tuli. “Nuclear Data Sheets for a = 239”. In: *Nuclear Data Sheets* 122 (2014), pp. 293–376. DOI: 10.1016/j.nds.2014.11.003.
- [18] B. Singh and E. Browne. “Nuclear Data Sheets for A=240”. In: *Nuclear Data Sheets* 109 (2008), pp. 2439–2499. DOI: 10.1016/j.nds.2008.09.002.
- [19] C. Nesaraja. “Nuclear Data Sheets for a = 241”. In: *Nuclear Data Sheets* 130 (2015), pp. 183–252. DOI: 10.1016/j.nds.2015.11.004.
- [20] Y. A. Akovali. “Nuclear Data Sheets for a = 242”. In: *Nuclear Data Sheets* 96.1 (2002), pp. 177–239. DOI: 10.1006/ndsh.2002.0011.
- [21] J. M. Verbeke, C. Hagemann, and D. Wright. *Simulation of Neutron and Gamma Ray Emission from Fission and Photofission*. UCRL-AR-228518. Lawrence Livermore National Laboratory, 2010. URL: <http://nuclear.llnl.gov/simulation/main.html> (visited on 02/20/2016).
- [22] R. T. Kouzes et al. “Cosmic-Ray-Induced Ship-Effect Neutron Measurements and Implications for Cargo Scanning at Borders”. In: *Nuclear Instruments and Methods in Physics Research Section A: Accelerators, Spectrometers, Detectors and Associated Equipment* 587.1 (Mar. 2008), pp. 89–100. DOI: 10.1016/j.nima.2007.12.031.
- [23] I. Jovanovic and A. S. Erickson, eds. *Active Interrogation in Nuclear Security*. Advanced Sciences and Technologies for Security Applications. Cham: Springer International Publishing, 2018. DOI: 10.1007/978-3-319-74467-4.
- [24] C. Hagemann, D. Lange, J. Verbeke, and D. Wright. *Cosmic-Ray Shower Library (CRY)*. UCRL-TM-229453. Lawrence Livermore National Laboratory, 2012.